

EXPERIMENTAL STUDIES OF ELECTRON BEAM FOCUSING WITH SOLENOID LENSES NEAR THE SPACE CHARGE LIMIT*

M. Reiser, W. Namkung, P. Loschialpo, J. Suter,⁺
and J. D. Lawson⁺⁺

⁺University of Maryland, College Park, Maryland 20742
⁺⁺Rutherford Laboratory, United Kingdom

Abstract. Experimental studies of beam focusing with the first solenoid lens in the University of Maryland electron beam transport experiment (at 5kV, 230-310 mA) are reported. At zero magnetic field, the density profile and beam envelope are in agreement with theory. When the beam is focused with the lens, it becomes hollow, develops halos near the waist, and shows images of the anode mesh downstream from the waist. When the diameter is reduced, the beam is less hollow, the halos are smaller and the images improved. These effects are attributed to lens aberration, nonlinear space-charge forces, beam rotation, and transverse velocity components.

Introduction and General Considerations

The motivation¹ for the Maryland-Rutherford electron beam transport experiment, design features², and preliminary results³ with two solenoid lenses were discussed in three previous papers. To repeat briefly, the main objective of our project is to study the causes of emittance growth and instabilities that limit the beam current and the brightness in a periodic focusing channel. Our initial goal is to understand the behavior of an unbunched, long beam in transverse phase space; the study could be extended later to the more complex case of a bunched beam.

The main impetus of our work is to check whether the instabilities predicted by recent theoretical and numerical studies^{4,5,6,7} can be observed experimentally. In addition, we want to study other effects that deteriorate the beam quality such as aberrations due to external fields and nonuniform space charge densities. An electron beam in the range of a few keV was chosen for reasons of small scale and low costs. Periodically spaced short solenoids are being used to focus the beam in the first phase of our project.

Theoretically, the radius, a , of a beam in a solenoidal focusing system is determined by the envelope equation (paraxial approximation, Larmor frame)

$$\frac{d^2 a}{dz^2} + \kappa(z)a - \frac{K}{a} - \frac{\epsilon}{3} = 0, \quad (1)$$

where $\kappa(z) = (qB/2m_0c\beta\gamma)^2$, $B = B(z)$ = magnetic field on the axis, $K = (I/I_0)(2/\beta^3\gamma^3)$ = generalized perveance, I = beam current, $I_0 = 4\pi\epsilon_0 m_0 c^3/q = 1.7 \times 10^4$ amperes for electrons, ϵ = (rms) emittance, q = particle charge, m_0 = rest mass, and $\gamma = (1 - \beta^2)^{-1/2}$.

When the focusing system is periodic, with period $\Delta z = S$, the beam physics is determined by the "tunes," or phase advances per period, σ and σ_0 , of the particle oscillations with and without space charge, respectively. Equation (1) can

then be solved by the smooth-approximation technique and, for a channel with acceptance α and matched conditions, one obtains the following relations^{8,9}

$$I = I_0 \frac{\beta^3 \gamma^3 \alpha \sigma_0}{2S} (1 - \epsilon^2/\alpha^2), \quad (2)$$

$$\alpha = \sigma_0 \frac{\bar{a}^2}{S} = \sigma_0 \frac{a^2}{S} G, \quad (3)$$

$$\frac{\sigma}{\sigma_0} = \frac{\epsilon}{\alpha} = \sqrt{1 + u^2} - u, \quad (4)$$

where \bar{a} = average beam radius, and $u = KS/(2\sigma_0\epsilon)$; graphs and formulas for the factor G can be found in Ref. 9.

For a source with brightness B , one has

$$I = B\epsilon^2, \quad (5)$$

and the actual beam current corresponds to the intersection of curves (2) and (5) as illustrated in Fig. 1. The acceptance α of a channel can be defined by a suitably placed hole of radius a . Any emittance growth will reduce the brightness and hence the beam current through the hole (see dashed curve in Fig. 1). A measurement of the beam transmission thus provides a first indication on the existence of instabilities or other effects. Further refinements require beam profile and emittance measurements.

Theory and numerical simulations^{4,5,6,7} predict quadrupole (envelope) instabilities when $\sigma_0 > 90^\circ$ and sextupole (third-order) instabilities when $\sigma_0 > 60^\circ$. There are also intensity thresholds, i.e., lower limits for σ/σ_0 , that depend on the form of the particle distribution function and on coupling between transverse and longitudinal modes. For a K-V distribution, for instance, one has the stability requirement $\sigma/\sigma_0 \geq 0.4$ and $\sigma_0 < 60^\circ$. In our experiment, we plan to vary both σ and σ_0 over a wide range to cover all possible instability modes predicted by theory. The use of grids² to accomplish this is being studied at the Rutherford Laboratory.

Electron Beam Apparatus

The three major components of the apparatus are the electron gun, the solenoid focusing system, and the diagnostic chamber, as described previously.³ The experiment is designed to proceed in stages: several electron guns producing different beam characteristics will be tried; the various beam profiles in free space are measured first; then solenoid lenses will be added, one at a time, until the full length of the focusing channel (approximately 30 lenses) is completed.

In preliminary studies with a home-made

*Work supported by DOE Contract #DE-AS05-78ER5940

electron gun, we measured the free-space beam envelope expansion and focusing with one and two lenses.³ Subsequent measurements of the radial current density with a Faraday cup revealed that the beam becomes hollow when it is focused. This led us to start a more systematic study of the beam properties with only one solenoid lens.

The experimental configuration for the measurements is shown in Fig. 2. The electron gun is the same as that in Ref. 3, except that the cathode-anode gap is only 1.6 cm and the beam current is 310 mA (versus 230 mA) at 5 kV. The diameter of the cathode is 1 cm and the anode aperture is covered with a fine tungsten mesh. The center of the solenoid is 8.6 cm from the anode. A fluorescent screen at the end of a hollow tube, can be moved along the beam axis; the screen pictures of the beam, which can be seen through the tube, are recorded with the aid of a TV video-tape system.

Experimental Results

The radial density profile near the anode, fluorescent screen pictures, and the beam envelopes for various peak magnetic fields (from 0 to 380 G) of the full-size beam were already published in our previous paper.³ We have now also measured the radial density profiles versus distance along the axis for various magnetic fields. Figure 3(a) shows three profiles at a distance of 20, 22, and 24 cm, respectively, with a fixed peak magnetic field of $B_0 = 117$ G. The most notable feature is the hollow structure of the profile even though the beam prior to entering the lens has a peaked, almost Gaussian, shape (see Ref. 3). However, it appears that with increasing distance, the hollow feature gradually disappears. The asymmetry in the profile curves is caused by misalignments in the system and possibly some nonuniformity in cathode emission.

We do not fully understand yet why the beam becomes hollow. However, qualitatively, we attribute this phenomenon to a combination of lens aberrations, nonlinear space charge forces, trajectory rotation in the solenoidal magnetic field, and the relatively low temperature of the beam. (The emittance is $\epsilon \geq r_c \sqrt{2kT/eV} = 3 \times 10^{-5}$ m-rad, where $r_c =$ cathode radius = 0.5 cm, $kT =$ cathode temperature ≈ 0.12 eV, $V =$ gun voltage = 5 kV).

From the qualitative analysis, one concludes that the radial profile should be less hollow when the beam radius is reduced since all of the mentioned effects increase with radius. We therefore inserted a thin mask into the beam behind the anode, with an aperture of 0.5 cm thus reducing the beam size by a factor of two. An important additional feature of the mask are two 0.5 mm pinholes outside of the reduced beam aperture but inside of the full-size beam radius, as shown in the upper left corner of Fig. 4.

We should note that the mask reduces the current I , and hence K , by a factor of 4 and the emittance by a factor of 2. Consequently, in a periodic channel, the space charge parameter u would decrease by a factor 2 and the tune shift ratio σ/σ_0 would increase.

Some experimental results obtained with the reduced beam are shown in Figs. 3(b), 4, and 5. First, in Fig. 3(b), we see, by comparison with 3(a), that the beam profile is considerably less hollow than in the case of the full-size beam confirming our expectations. In Fig. 4, the envelopes for the reduced beam are plotted for different magnetic fields. Computations show that only the free-space curve ($B_0 = 0$) agrees with the envelope obtained from integration of Eq. (1). The phosphor screen pictures taken at a fixed axial position of $z = 16$ cm with varying magnetic field strength, are seen in Fig. 5. We note that all of the features discussed already in Ref. 3 are present here as well, in particular, halos near the waist and images of the anode mesh downstream from the waist. However, in contrast to the full-size beam, the halos are less pronounced and the images are sharper. Of particular interest is the fact that the images of the anode mesh first show shadows of the wires; but then, as the magnetic field is increased, they become bright.

Equally noteworthy is the behavior of the two beamlets defined by the pinholes. Since they are launched from a region outside of the reduced beam radius, the defocusing force due to the space charge ($F \propto I/r$) is less than on beam electrons near the edge ($r = a$). Thus, the two beamlets enter into the beam (near $z \approx 18$ cm), as indicated schematically in Fig. 4 for the outer beamlet, (b). When the magnetic field is turned on and increased, the two beamlets cross the axis and emerge on opposite sides of the beam, as can be seen in the photos of Fig. 5. One can also see a coma-like distortion of the beamlet cross section.

In conclusion, we found that the beam, focused by only one solenoid, shows a variety of effects some of which were unexpected. While we do have some qualitative explanations, more experimental studies as well as numerical simulation will be required to obtain a full understanding. Thus, in parallel with the construction of the periodic solenoid channel, we plan to devote some time to more detailed studies of beam behavior in a single lens.

With regard to the periodic channel, we plan to increase the effect of emittance versus space charge, and thus the tune σ , by lowering the gun voltage, decreasing the beam perveance, and using beam masks and special grids. The first results with the grids at the Rutherford Laboratory are already quite encouraging: it was demonstrated that the beam radius can be increased easily by a factor of two with proper grid voltage and polarity.

References

1. M. Reiser, W. Namkung, and M. A. Brennan, IEEE Trans. NS-26, 3026 (1979).
2. M. A. Brennan, P. Loschialpo, W. Namkung, M. Reiser, and J. D. Lawson, Proc. Heavy Ion Fusion Workshop, LBL-10301, Oct. 1979, p. 77.
3. W. Namkung, P. Loschialpo, M. Reiser, J. Suter, and J. D. Lawson, IEEE Trans. NS-28, 2519 (1981).

4. L. Smith et al., HIFAN-13, 14, 15, and 43, Lawrence Berkeley Laboratory (1977).
5. I. Haber and A. W. Maschke, Phys. Rev. Lett. 42, 167 (1979).
6. I. Hofmann, IEEE Trans. 28, 2399 (1981).

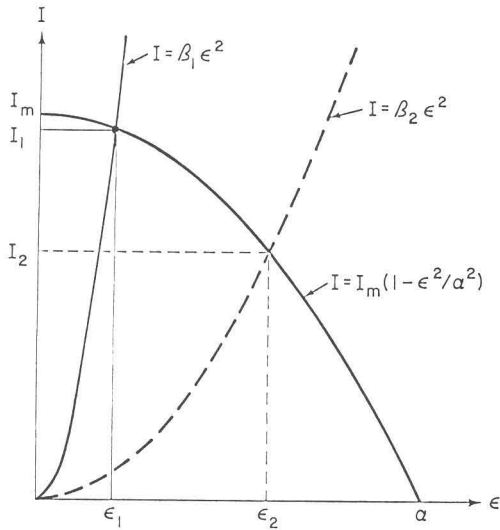


Fig. 1 Channel acceptance, Eq. (2), and brightness, Eq. (5), define actual beam current, I_1 ; $I_m = 0.5 I_0 \beta^3 \gamma^3 \alpha \sigma / S$, $B_2 < B_1$.

7. T. F. Wang and Lloyd Smith, IEEE Trans. NS-28 2477 (1981).
8. M. Reiser, Part. Accel. 8, 167 (1978).
9. M. Reiser, J. Appl. Phys. 52, 555 (1981).
10. J. D. Lawson and D. H. Reading, private communication.

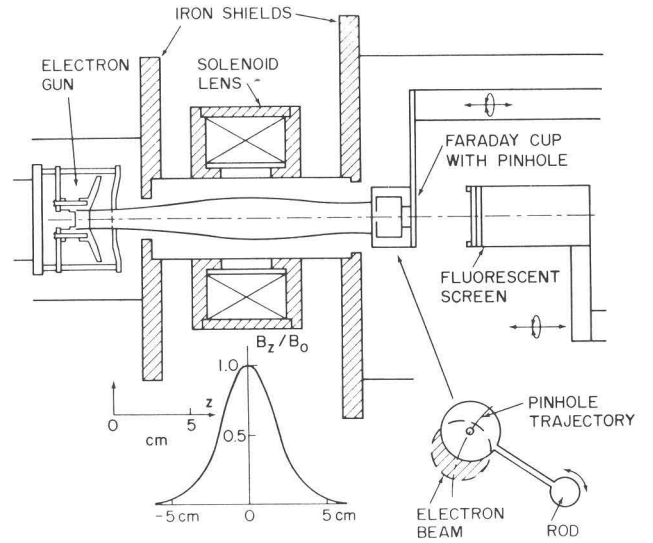


Fig. 2 Experimental setup with magnetic field profile.

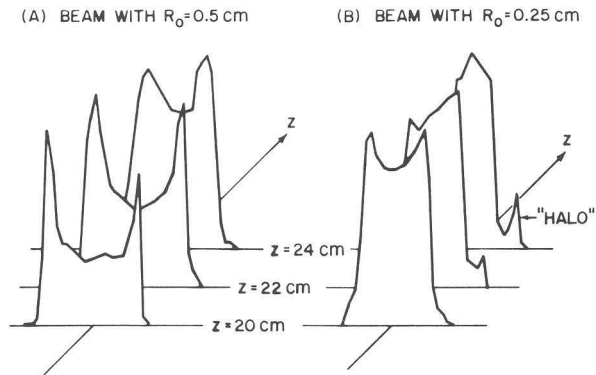


Fig. 3 Radial density profiles for full-size (a) and half-size (b) beam at $B_0 = 117$ G, $V = 5$ kV.

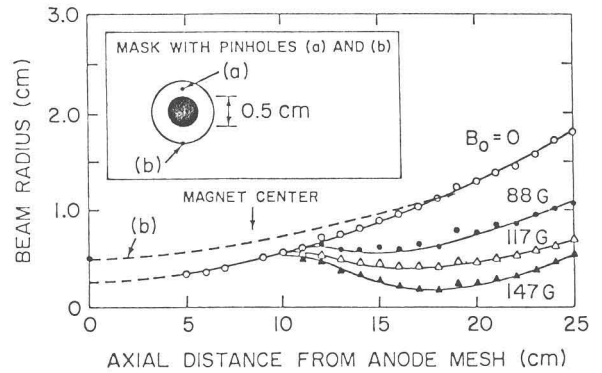


Fig. 4 Envelopes at various magnetic fields for reduced beam size. Insert shows beam mask with two pinholes.

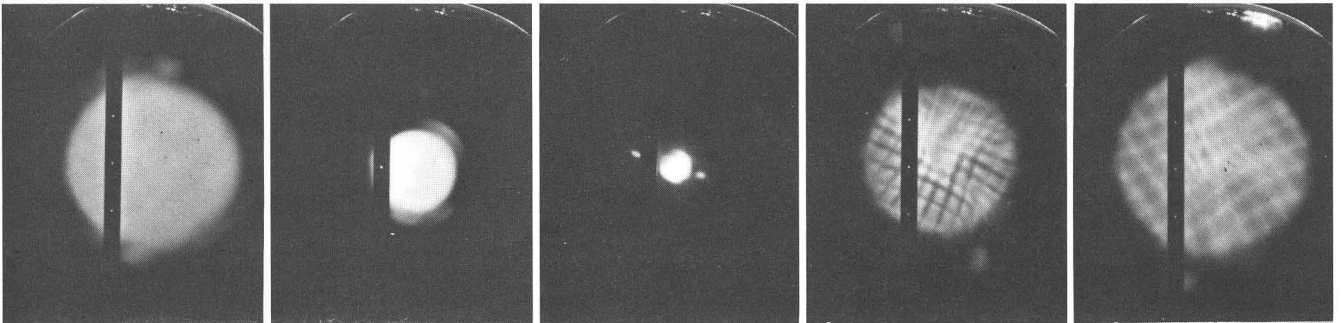


Fig. 5 Phosphor screen pictures at $z = 16$ cm for $B_0 = 0, 117$ G, 176 G, 264 G, and 322 G.

Discussion

The experimental beam envelope curves show that violent effects occur when the beam radius is only 40% of the lens radius. (1 cm out of 2.5 cm.) The experimental envelopes agree with integration of the envelope equations only without the magnetic field. So there is more physics than the envelope equations contain, and we hope to get that from numerical simulations.

We started with a solid beam and see hollowing and later reforming to a core again. If one wanted to use the higher space-charge limit of the hollow beam, one should start with an injected hollow beam.